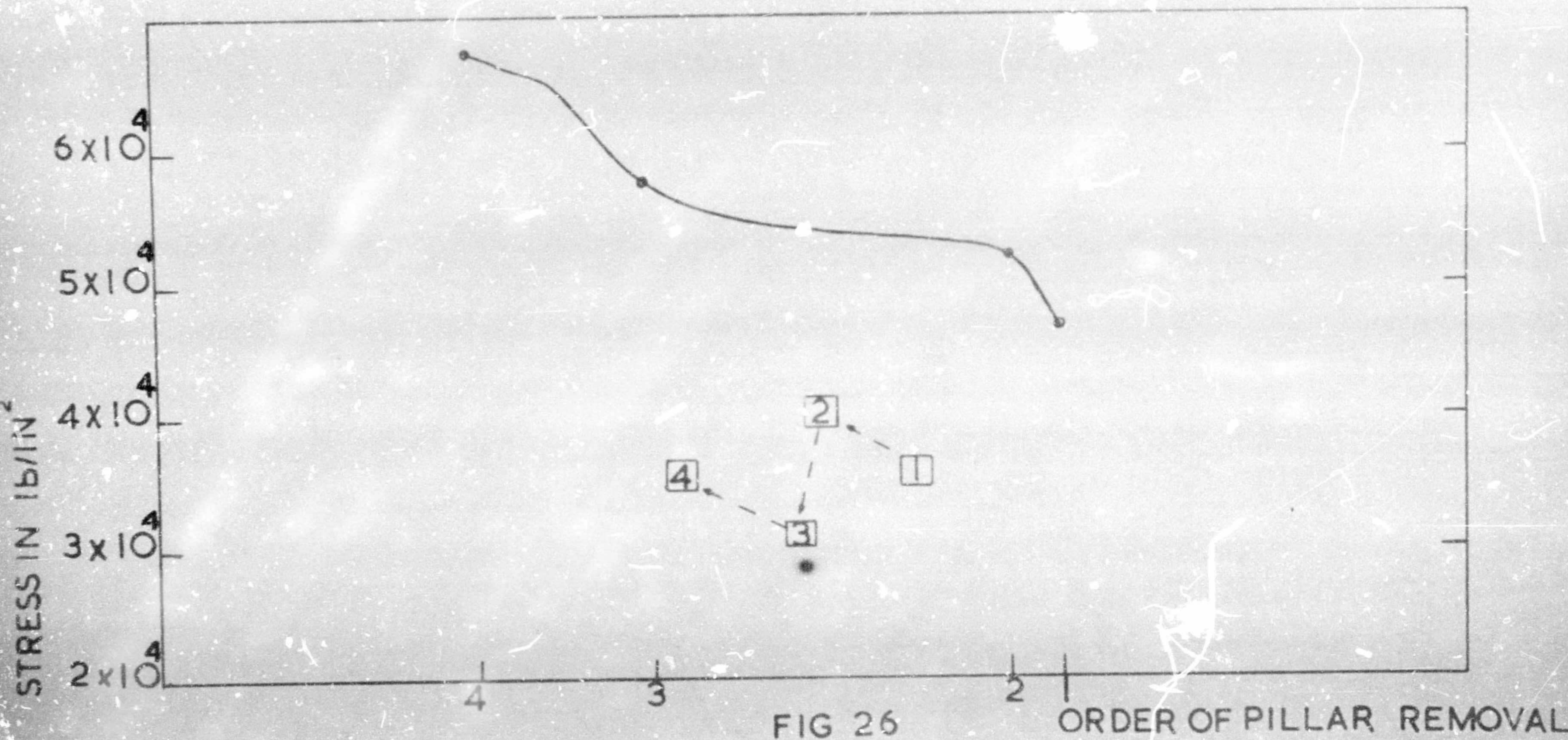

FIG 26

STRESS IN PILLAR No 4 AS THE OTHER PILLARS ARE REMOVED

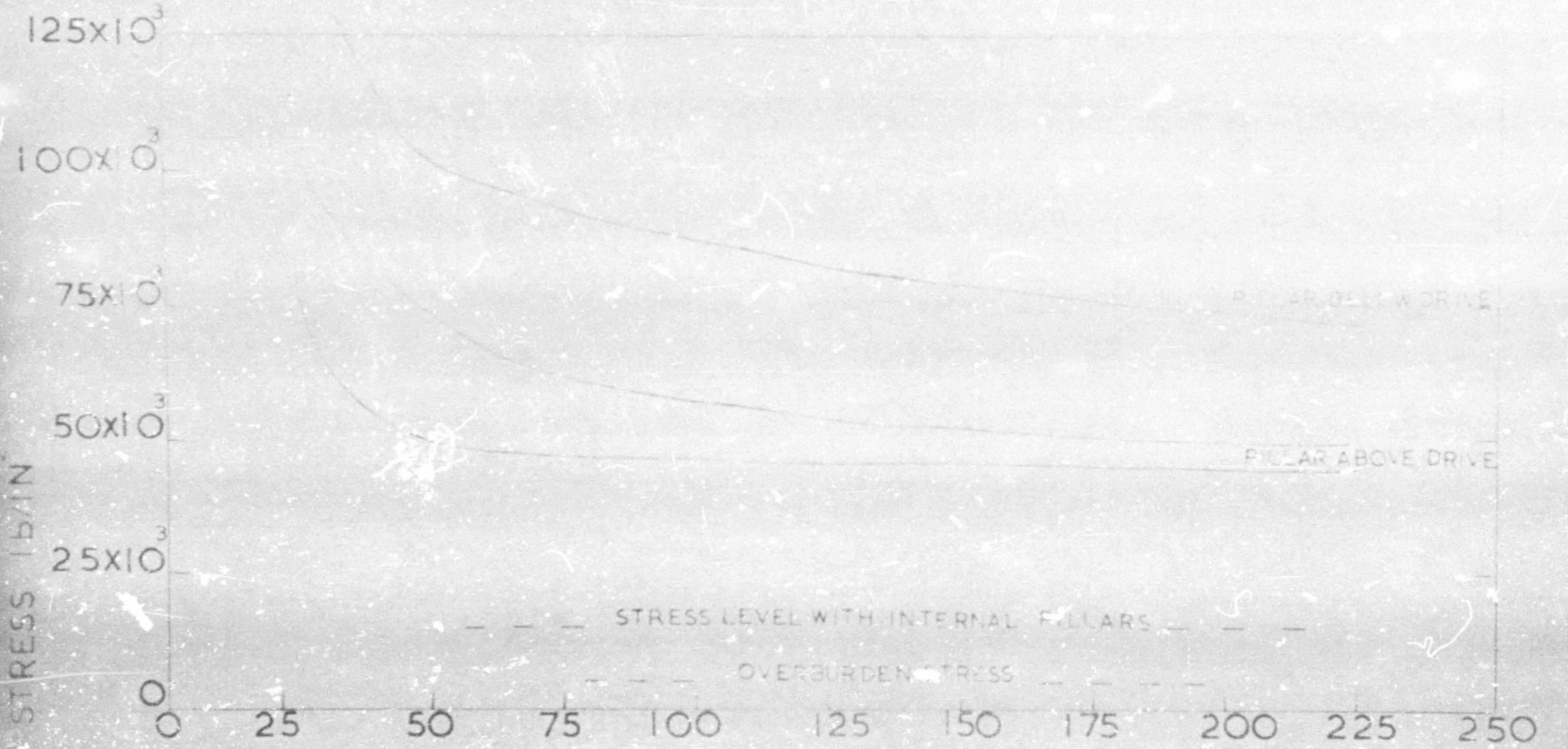

FIG 27

STRESS CHANGE AT A POINT IN THE DRIVE PILLAR

AS THE PILLAR FACE APPROACHES

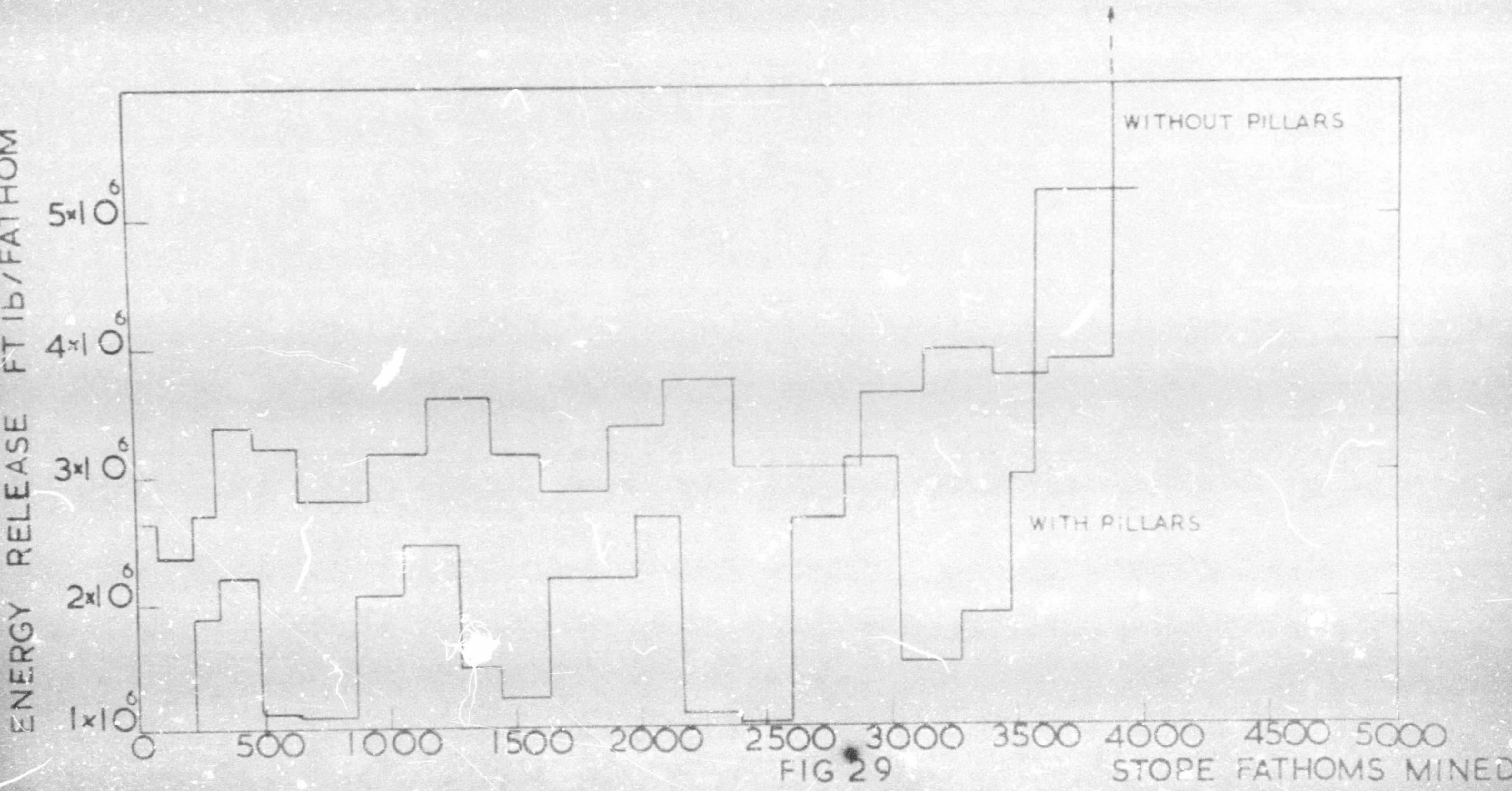

FIG 29

ENERGY RELEASE MINING WITH AND WITHOUT PILLARS

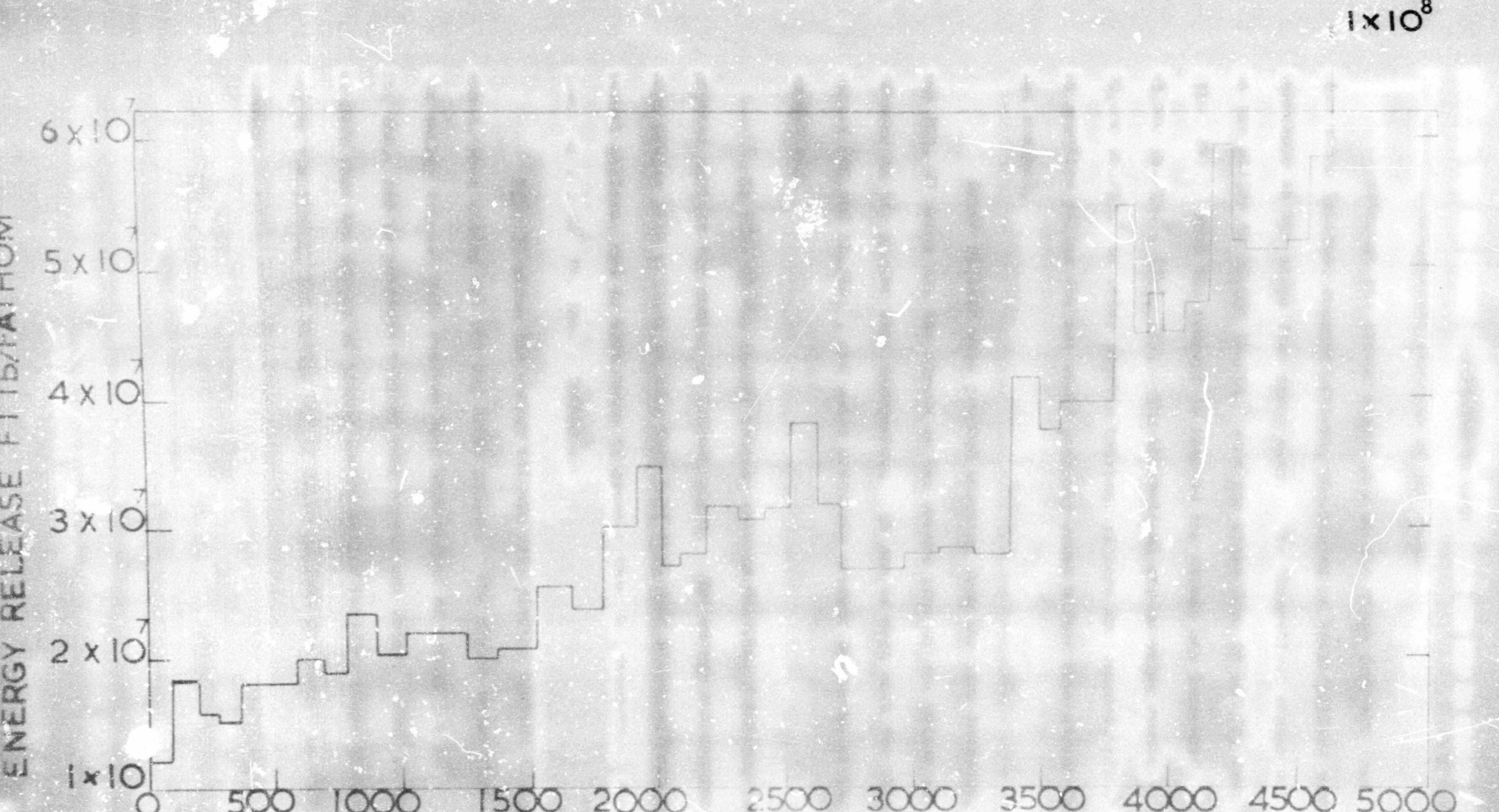

FIG 30

ENERGY RELEASE WHEN MINING OUT THE DRIVE PILLARS

pillars, but the stress magnitudes in both cases are now in excess of the uniaxial compressive strength of the rock.

Although the stress magnitudes on the stope face are less when using internal support pillars, the stress on these pillars rapidly increases as the stope face moves away. The theoretical stress value on the pillar is 20,000 lb./in.^{2} when the stope face is 100 ft. away, (FIG. 24). When the remnant is removed the stress has increased to 48,000 lb./in.^{2}, (FIG. 25). The theoretical stress value reaches 70,000 lb./in.^{2} as other payable internal pillars are removed, (FIG. 26) In practice pillar failure would probably occur before this stress level was reached.

Drive pillars were removed starting from the mine boundary, and FIG. 27 shows how the stress on the centre line of the pillar increases as the pillar face approaches. It can be seen that the stresses exceed 100,000 lb./in.^{2}, and would certainly produce dangerous mining conditions.

In FIG. 29 the energy release rate in ft. lbs. / fathom, is plotted against the number of fathoms mined. The energy release rate when mining [illegible] less than half that when mining without internal pillars, [illegible] cases is greater than the theoretical danger level of 2 x 10^5 ft. lbs. / fathom^5.

FIG. 30 shows the energy release rate plotted against fathoms mined, when mining out the top drive pillar. The figure shows that the energy release rate reaches very high values of almost 1 x 10^8 ft. lbs., and in practice violent rock bursts may occur. Thus it can be seen that the system of mining incorporating internal stope pillars may be beneficial, but mining out of drive pillars can result in rock bursts.

TABLE 1

SPECIMEN NUMBER	ROCK TYPES	DYNAMIC MODULUS Ed. x 10^6 lb./in.^{2}	STATIC RESULTS YOUNG'S MODULUS lb./in.^{2}	PERCENTAGE DIFFERENCE BETWEEN RESULTS	PERCENTAGE DIFFERENCE SAME GEOLOGICAL TYPE
1	Footwall	10.5			
2	Quartzite	11.6	11.6 & 11.3	Nil	9.5
3	Basal	11.5			
4	Reef	10.3			
4A	Quartzite	9.8	8.1 & 9.1	12	29
5		9.7			
6		9.7	10.4	7	
7	Middling	10.2			
8	Quartzite	9.2	8.5 & 9	3.5	17
9	Hangingwall	8.8			
10	Quartzite	8.8	7.8 & 7.6	12.5	
11		6.7			55
12		10.2			
13		9.3			
14		11.1			
15	Ventersdorp	10.6	11.7 & 12.2	12	15
16	Sediments	10.6			
17	Dyke	13	12.9 & 13	Nil	
18		15.9	15.0 & 15.3	4.5	18
19		14.4			

TABLE 2

SPECIMEN NUMBER	ROCK TYPES	CORE SIZE	FAILURE STRESS	POISSON'S RATIO	YOUNG'S MODULUS
1	B/R	BX	37,800	0.123	11.05
1A	B/R	BX	42,600	0.187	11.59
2	B/R	BX	-	0.156	11.7
3	F/W	BX	31,000	0.144	13.8 H
4	B/R	BX	32,100	0.137	11.82
6	B/R	NX	36,800	0.112	11.27
7	F/W	NX	29,150	0.132	11.72
8	B/R	NX	-	0.142	11.50

Average Values: Young's Modulus = 11.52 x 10^6

Poisson's Ratio = 0.142

Range of Failure Stress 27,000 lb./in.^{2} to 43,000 lb./in.^{2}

H Faulty Gauge

B/R Basal Reef Quartzite

F/W Footwall Quartzite

6. UNDERGROUND TESTS

The objectives of the underground tests were to determine :-

(1) The behaviour of stope pillars by measuring stress within the pillar and closure at the pillar sides;

and

(2) The effect of pillars on strata movement by measuring closure and ride in the stope excavation and around the drives, before and after pillar extraction.

The first set of tests was carried out in 2323 Stope, since the stope pillars were ready for removal. Closure and ride measurements were made as stress measuring equipment was not available. The results of the tests were compared with the results obtained on the Resistance Analogue. This comparison indicated that pillars had already failed. It was realised then that a more comprehensive programme was necessary to determine when failure occurred, and that closure and stress measurements would be required from the commencement of pillar formation. For this purpose 2436 Stope was chosen, and closure measurements were made until stress measuring equipment arrived. Measurements of stress in 2436 Stope and later in 2426 Stope showed considerable limitations in the stress measuring equipment used.

6.1 Measurement of Stress:

Initially it was intended to use electrical resistance strain gauge equipment for stress measurement, but after discussion with the Rock Mechanics Research Team of the C.S.I.R. it was found that the commercially available equipment was not reliable. It was therefore decided to use photo-elastic strain gauge equipment, which was considered to be reliable, and was commercially available[14].

Photo-elastic strain gauge equipment depends on the property of a bi-refringent material to show changes of strain, (Sec. 5.2). A hand-held polariscope is used to read the isochromatic fringe pattern formed in the gauge. A description of the photo-elastic gauge used in

"in-situ" / ......

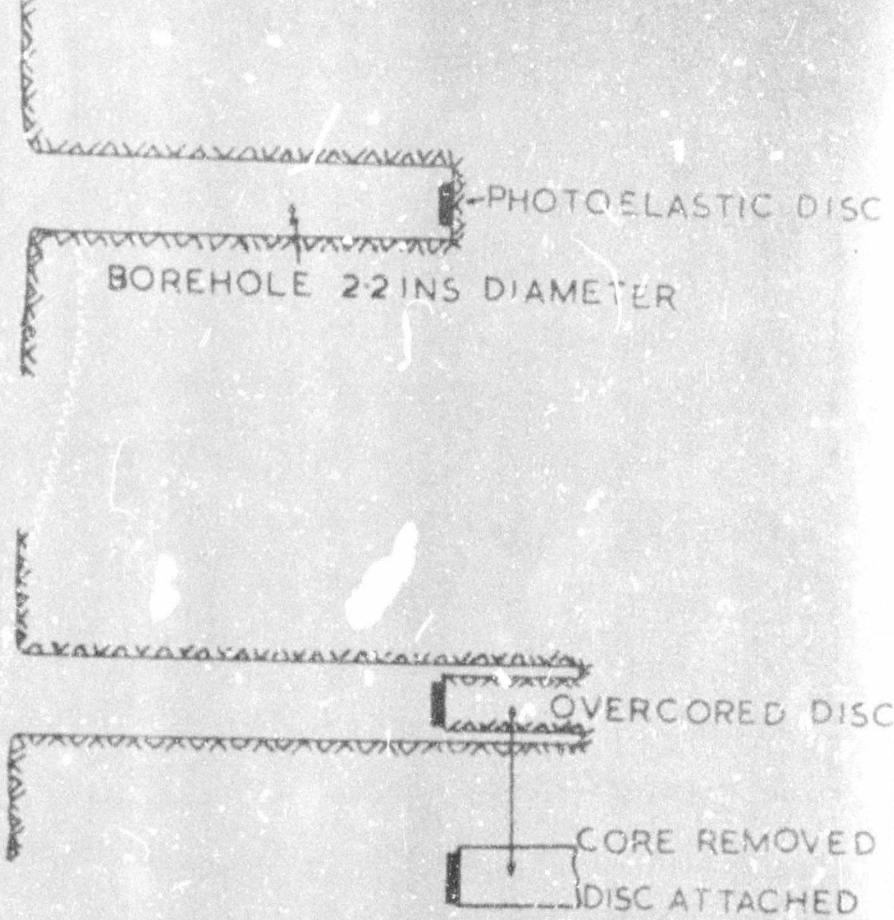

FIG 31A

OVERCORING

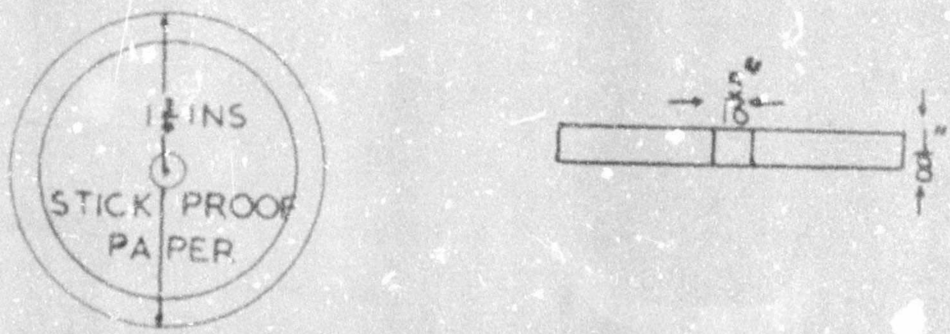

FIG 31b

THE PHOTOELASTIC DISC

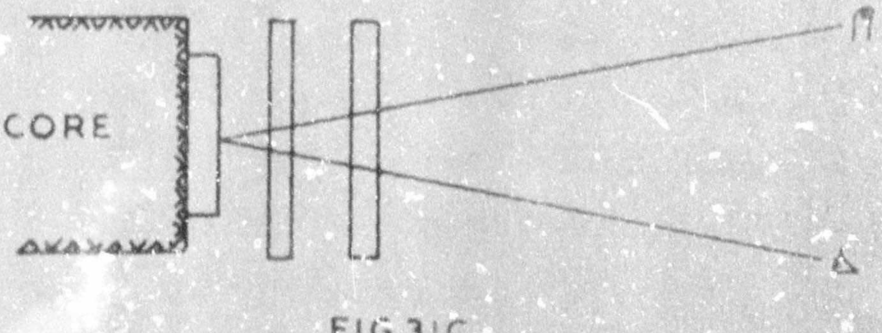

FIG 31C

THE HANDHELD POLARISCOPE

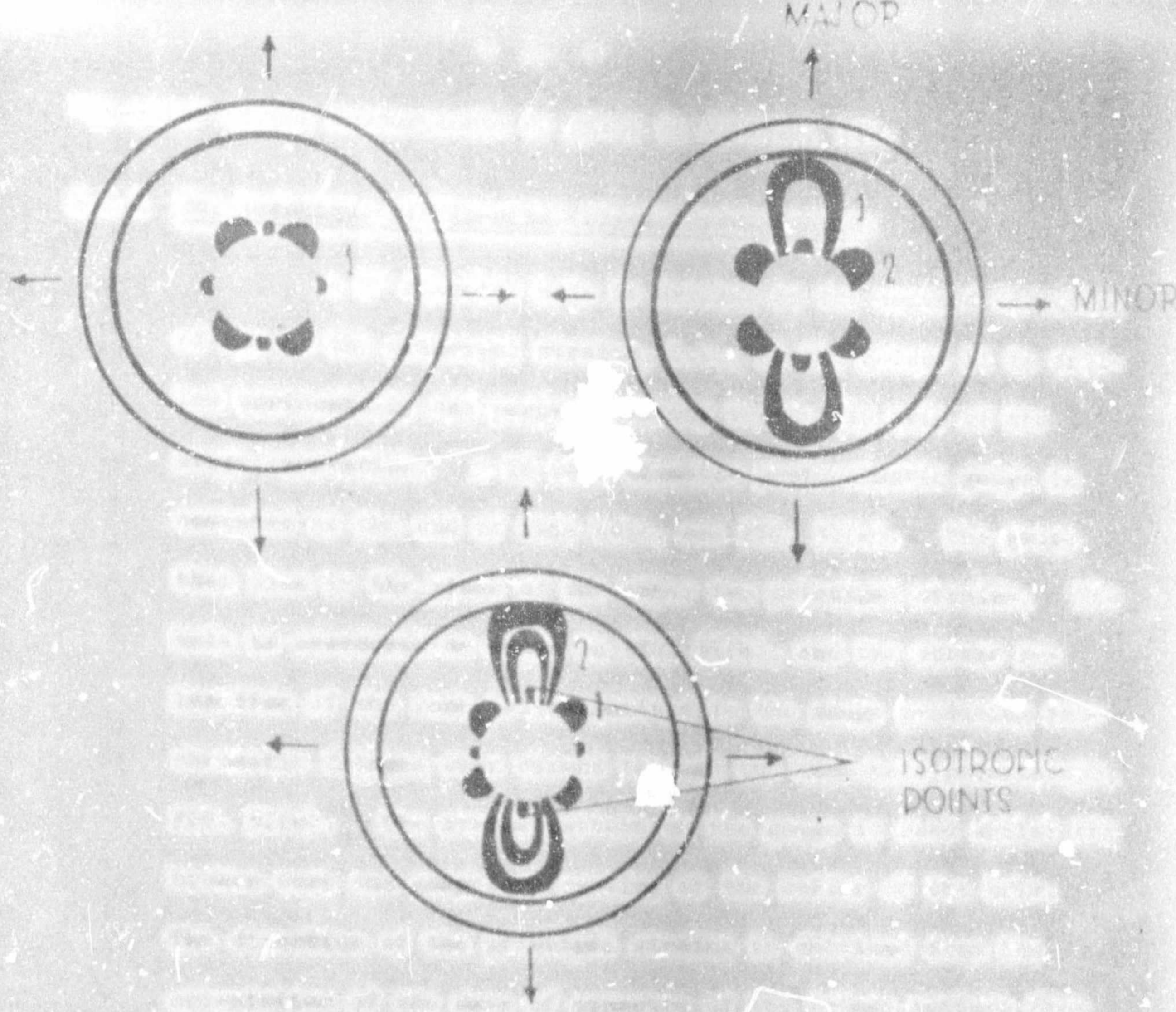

URE 37 (A) FRINGE PATTERNS STRAIN RATIO +1 1/4

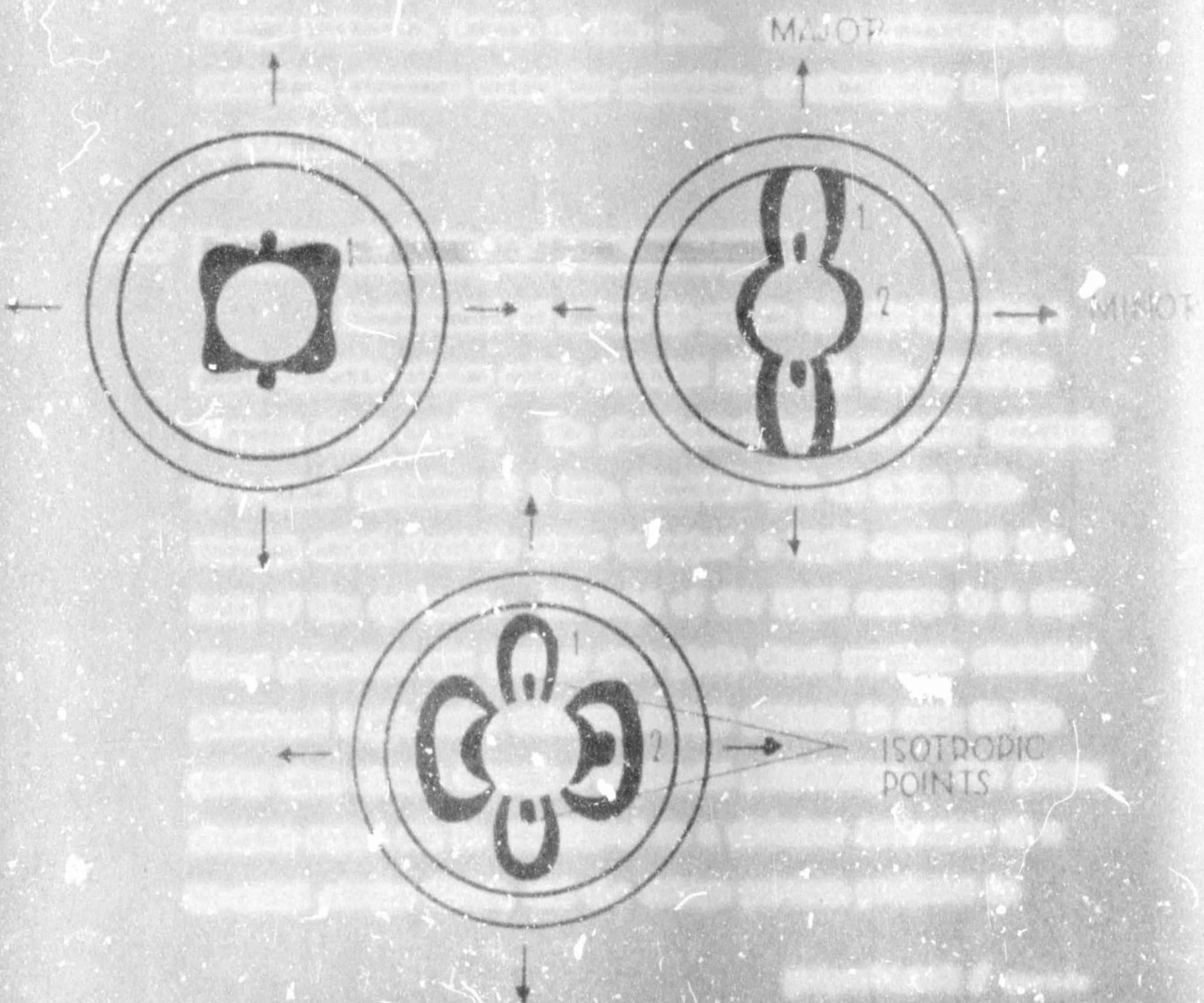

"in-situ" stress measurements is given in APPENDIX III.

6.1.1 The Technique of "In-situ" Stress Measurements:

A 2" diameter hole is drilled in the assumed direction of one of the principal strains, i.e., at St. Helena it is drilled horizontally and perpendicularly to the dip axis of the stope excavation. A 1¼ ins. diameter photo-elastic gauge is cemented at the end of this hole, see FIG. 31(a). The gauge then lies in the plane of the other two principal strains. The hole is overcored as shown in FIG. 31(b), and the stress relaxation of the rock is transmitted to the gauge producing isochromatic fringes when viewed through the hand-held polariscope, FIG. 31(c). The stress pattern on the gauge is read whilst the broken core and gauge are resting at the collar of the hole. The direction of the principal strains is obtained from the orientation of the axes of symmetry of the fringe pattern from a vertical reference line. The magnitude of the strains is determined by a comparison with a set of standard whole number fringe patterns, (shown in FIG. 32). The determination of the principal stresses using the equations of elasticity is given in APPENDIX III.

6.1.2 Technique of Change in Stress Measurement:

Measurement of change in stress is made by using a photo-elastic stress meter cemented into a 1½ ins. diameter diamond drill hole[15]. The photo-elastic stress meter consists of a glass cylinder of 1 ins. diameter with an axial hole through which electric wires energise a light source at the back of the cylinder. In front of the light source is a combined polarizer and quarter wave plate which produces circular polarized light and a coloured fringe pattern is seen in the meter when viewed through a hand-held polariscope. The photo-elastic meter can be considered as a circular inclusion in a bi-axial stress field, and the fringe pattern produced is

proportional / ......

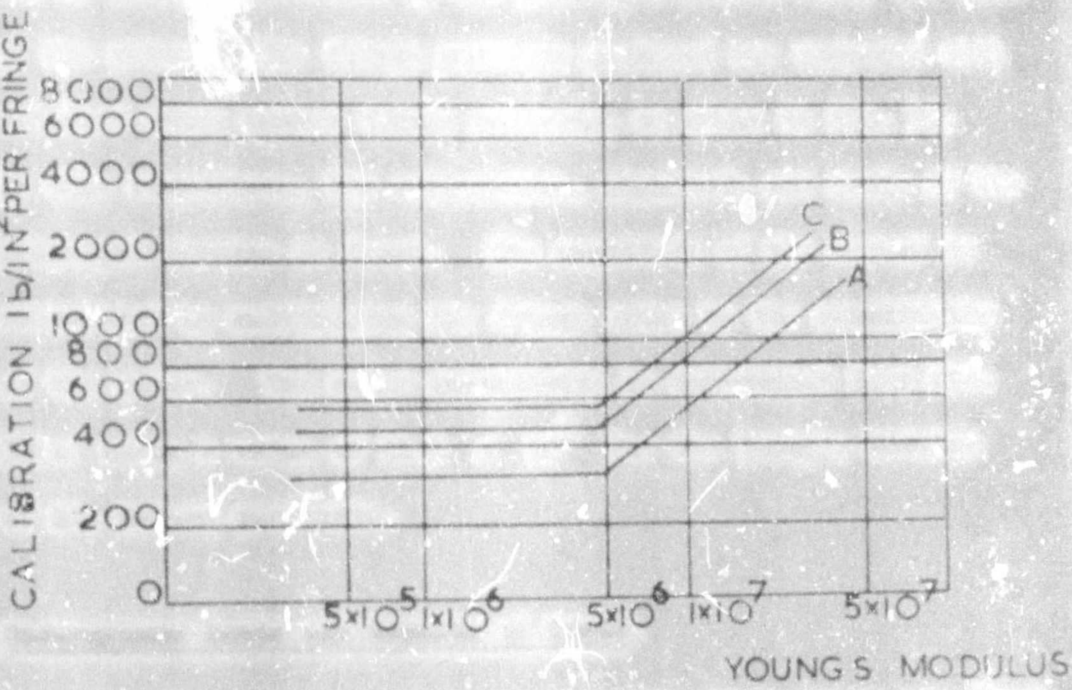

FIG 33A

THE EFFECT OF THE MODULUS OF ELASTICITY OF THE SURROUNDING MATERIAL UPON THE CALIBRATION CHARACTERISTIC OF THE STRESSMETER

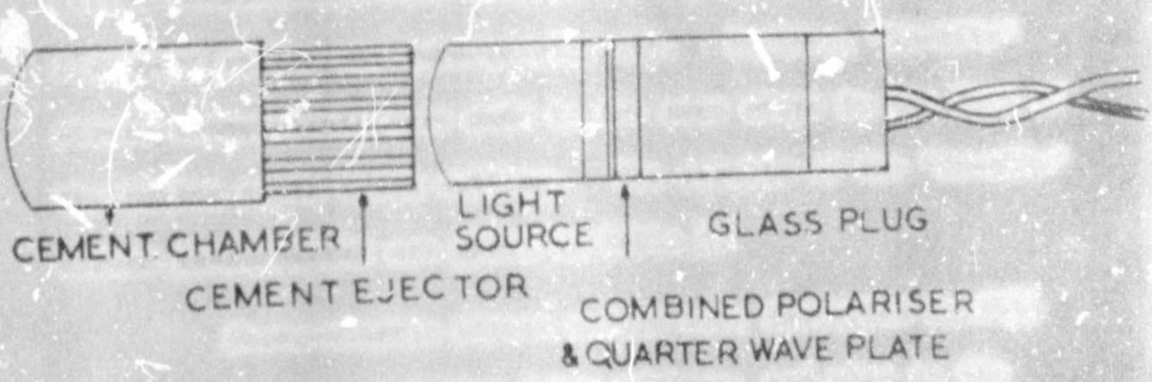

FIG 33b

THE PHOTOELASTIC STRESSMETER

proportional to the principal stress in the plane of the meter and is almost unaffected by the principal stress along the axis of the meter. The fringe patterns produced are compared with standard whole number fringe patterns, as shown in FIG. 32. By this comparison, the orientation, magnitude and ratio of the principal strains is found. The magnitude of the stress is calculated by multiplying the fringe order by the sensitivity of the meter. The meter sensitivity is determined from FIG. 33(a) using a value of 11.5 x 10^6 for the Young's Modulus of St. Helena quartzite.

6.1.3 Underground Tests and Results of Tests:

The equipment for measuring "in-situ" stress was first tried out in 18 South Drive main development end at a depth of 4,000 ft. from surface. No trouble was experienced with the use of the equipment and it was possible to make three stress measurements in one diamond drill hole in eight hours. The results in 18 South Drive showed that the major principal stress attained a maximum value of 2,300 lbs./ins.^{2} at a depth of 4½ ft. from the collar of the hole. The angle between the direction of the principal stress and the vertical was 23°. Stress measuring equipment was then taken to 2436 Stope and "in-situ" stress measurements were made in the top north stope face where a support pillar was subsequently cut. Further, "in-situ" stress measurements were made in the same stope in the face of the bottom south track cutting. The results of the "in-situ" stress measurements are given in Table 3.

Photo-elastic stress meters were installed in 2436 Stope in the top and bottom drive pillars, and also in the internal pillars, (FIG. 45). The photo-elastic stress meter in the top North internal stope pillar was installed at a depth of 12 ft. ahead of the stope face at the centre of the future pillar. In this test the diamond drill hole was uncased and when the number of isochromatic fringes exceeded

six / ......

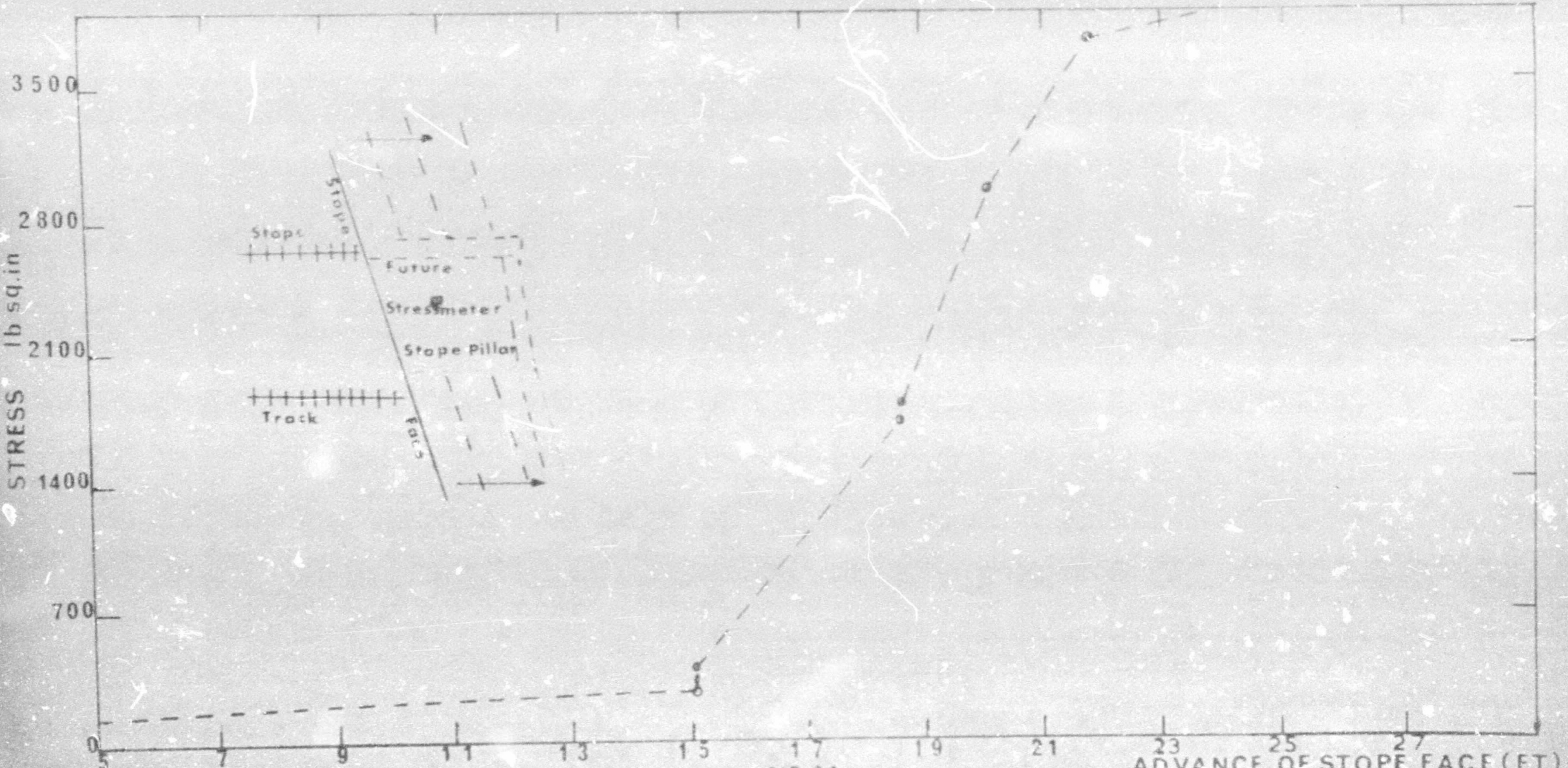

FiG 34

Stress Increase in the Stope Pillar as it is Being Formed

2436 Top North Pillar

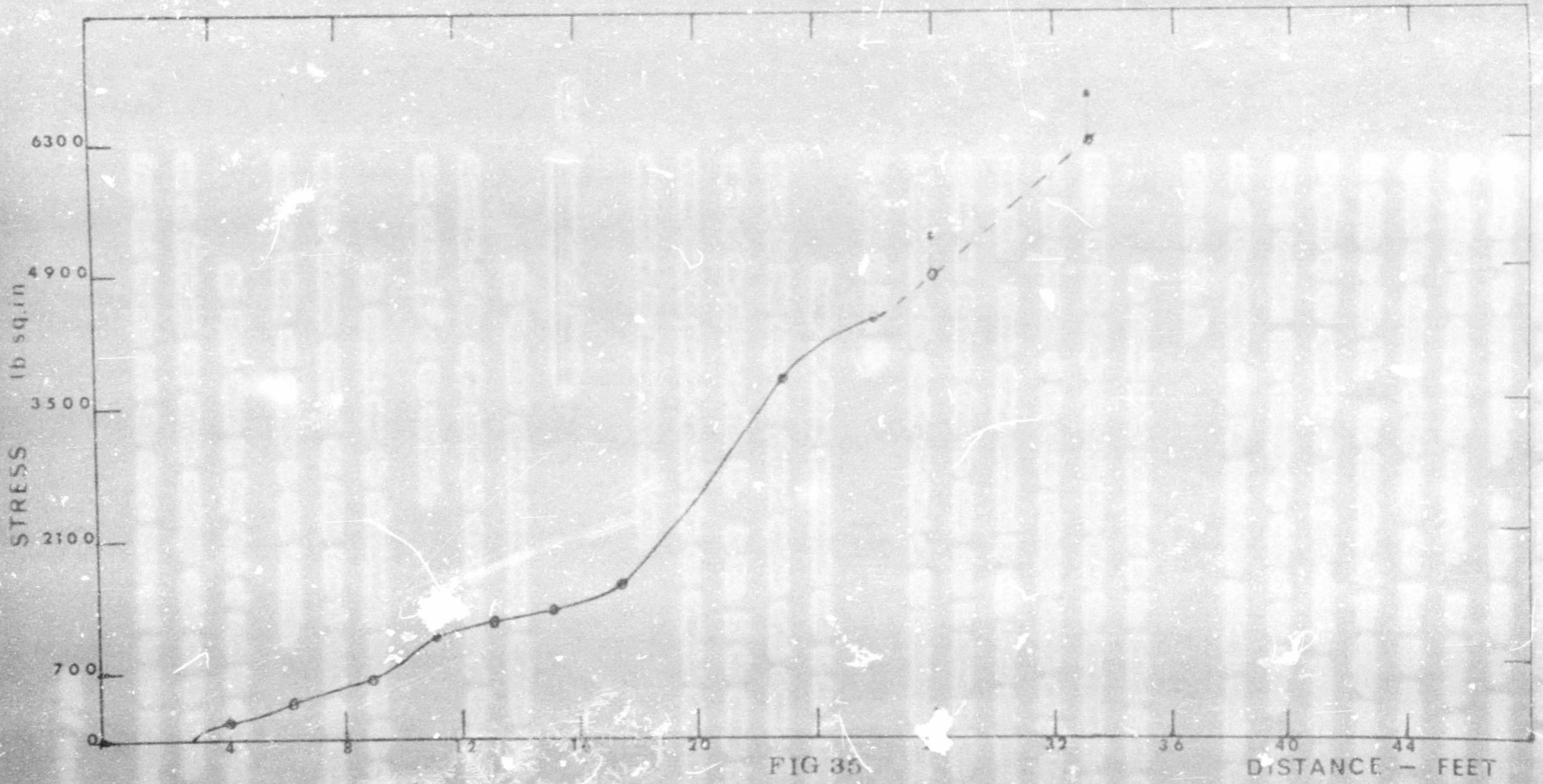

FIG 35

Stress Increase in the Drive Pillar as the Stope Face Advances

2436 Bottom South Drive Pillar

six, fracturing of the hole occurred preventing the further reading of the stress meter. At this stage the development of the pillar was only partly completed. The stress change plotted against the distance of the stope face from its original position is shown in FIG. 34. The direction of the major principal stress as given by the symmetry of the photo-elastic pattern was 40° from a vertical line through the axis of the meter. A comparison of the results with the Resistance Analogue results is given in FIG. 37.

The stress meter installed in the bottom South drive pillar in 2436 Stope recorded more than ten isochromatic fringes and the direction of the major principal stress was 3° from the vertical. Stress change measured by this meter and plotted against the distance from the stope face is shown in FIG. 35. A comparison with results obtained on the Resistance Analogue is given in FIG. 36.

Change in stress measurements made in No. 1 Stope pillar in 2426 stope are plotted against total closure at the edges of the pillar in FIG. 49. In FIG. 38 the change in stress results plotted against time are compared with results obtained on the Resistance Analogue.

6.1.4 Discussion of Results:

The "in-situ" stress measurements indicate that the direction of the major principal stress ahead of the stope face lies within 30° of the vertical.

The results show the relationship between the stress and the distance ahead of the stope face at which the measurement was taken, was similar in each borehole.

The first three to four feet of rock in each borehole was so fractured that stress readings could not be taken. From four feet to nine feet the stress increased to its maximum value,

and / ......

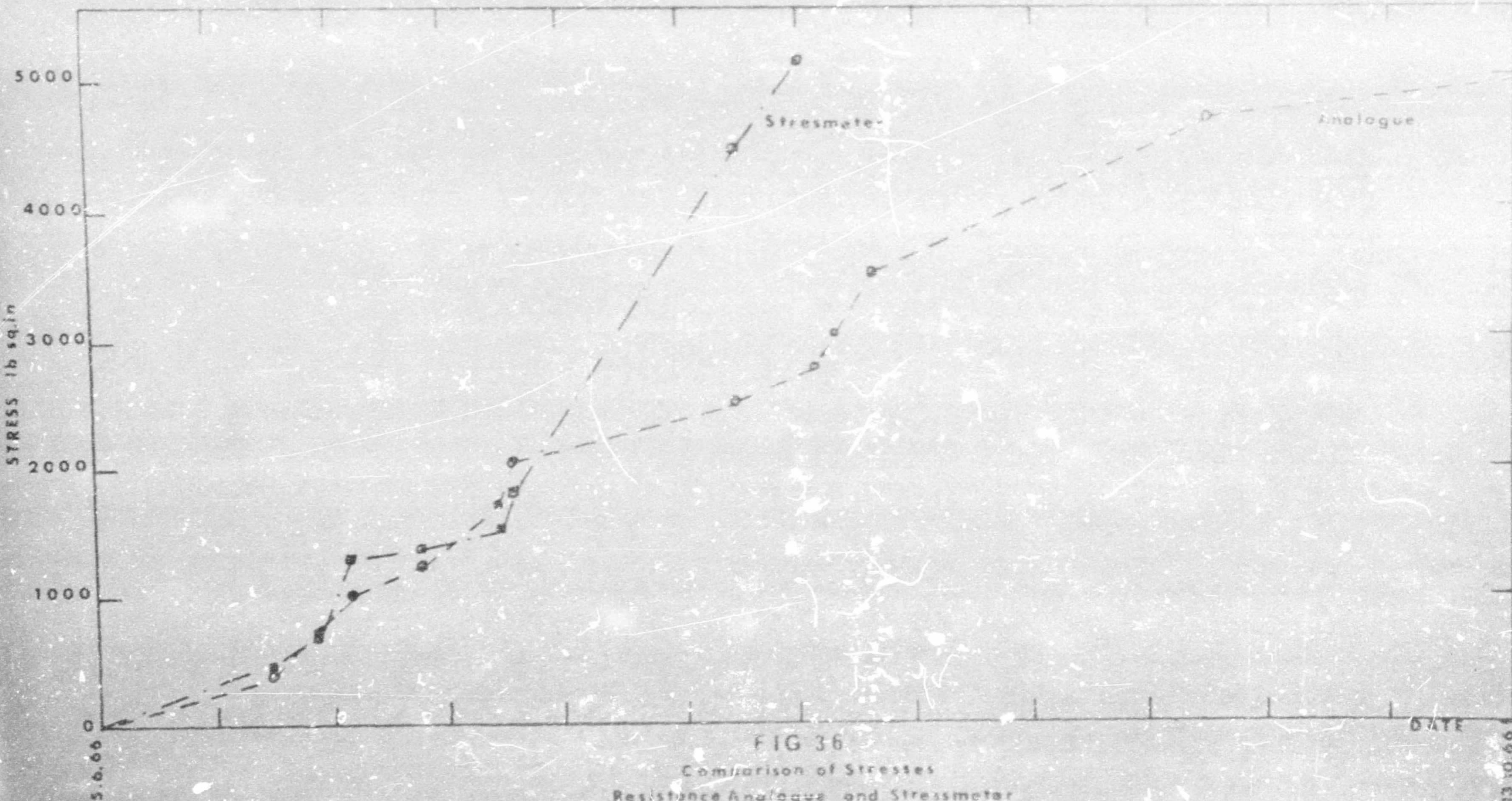

FIG 36
Comparison of Stresses
Resistance Analogue and Stressmeter
2436 Bottom Drive Pillar